

Biomimetic Design and Optimization of a Post-Earthquake Rescue Vehicle Inspired by Mole Cricket

Ting Cai¹, Lifu Liu^{2*}

¹College of Mechanical and Transportation, Southwest Forestry University, Kunming 650224, China

²Art and Design College, Southwest Forestry University, Kunming 2 650224, China

Received 15 Sep 2025

Accepted 12 Feb 2026

Abstract

To address the poor maneuverability and single-function limitations of traditional machinery in unstructured post-earthquake environments, this study proposes a novel systematic design framework integrating the Analytic Hierarchy Process (AHP) with biomimetic engineering. First, AHP was utilized to quantitatively prioritize diverse functional requirements, identifying "Passing" and "Rescue" as the dominant design constraints. Guided by these priorities and the principle of environmental isomorphism, the mole cricket was selected as the optimal prototype. Its biological features were mapped to engineering modules: the fossorial forelimbs were transformed into a hydraulic dual-end excavation system, and the segmented abdomen was evolved into a variable-volume telescopic tail warehouse. Finally, finite element modal analysis was conducted to verify dynamic feasibility. Structural optimization targeting the chassis and tail increased the first-order natural frequency from 9.03 Hz to 13.93 Hz, representing a 54.27% improvement. These quantitative results confirm that the optimized design effectively avoids low-frequency resonance and meets structural stiffness requirements, providing a robust theoretical blueprint for next-generation high-mobility rescue platforms.

© 2026 Jordan Journal of Mechanical and Industrial Engineering. All rights reserved

Keywords: Bionics design, Post-earthquake rescue vehicle, Analytic Hierarchy Process (AHP), Characteristics of mole crickets.

1. Introduction

Post-disaster rescue operations face extreme challenges under complex geological conditions. Disaster sites are typically characterized by paralyzed transportation networks, extensive structural collapses, and loose granular terrain. Currently, the main equipment used for post-disaster rescue is traditional construction machinery such as loaders and excavators. [1]. However, these machines are typically bulky and single-functional, lacking the necessary maneuverability to navigate narrow, unstable ruins effectively [2]. Consequently, the development of a specialized rescue vehicle that integrates high mobility, multi-functionality, and environmental adaptability has emerged as a critical research objective.

A systematic review of existing literature reveals that current research on rescue vehicles primarily focuses on three categories, each characterized by distinct limitations. The first category predominantly involves the modification of traditional engineering vehicles [3]. A typical approach is to integrate multi-functional tools (such as cutting and demolition devices) onto existing platforms to enhance task versatility. However, the inherent bulkiness and high chassis rigidity of traditional platforms limit their mobility in deep disaster zones, making it difficult to access narrow

or uneven rescue environments. The second category shifts towards small-scale biomimetic robots. In recent years, multi-legged or multi-segmented robots (such as crawlers inspired by centipedes or spiders) have demonstrated superior obstacle-surmounting capabilities on complex terrains, achieving adaptive obstacle crossing [4]. However, these robots generally suffer from limited load-bearing capacity and lack sufficient excavation or lifting power, rendering them unsuitable for heavy-duty tasks such as transporting wounded personnel or clearing large debris. The third category involves biomimetic vehicle design at the conceptual level. In recent years, biomimetic design has been regarded as a frontier pathway for enhancing the performance of rescue vehicles [5], [6]. Researchers often proceed from aesthetic appeal or ergonomics, proposing multi-modal platforms that emphasize visual and interactive biomimetic features [7]. Klyusov et al. proposed and designed a vehicle shape and chassis structure based on polar animals such as Arctic foxes and owls, achieving high maneuverability and reduced energy consumption in extremely low-temperature environments [8]. Estêvão and Araújo report details a study on a streamlined vehicle body inspired by box-shaped fish, which aims to reduce air resistance and enhance the stability of rescue vehicles when traveling at high speeds [9]. The report compares this design with traditional designs and confirms that the

* Corresponding author e-mail: llf665@126.com.

aerodynamic shape mimicking fish can significantly improve rescue efficiency. Nevertheless, most of these works remain at the level of "morphological mimicry" and lack systematic research on "functional translation" The design process relies on subjective intuition and fails to establish a quantitative decision-making framework to balance conflicting requirements such as speed versus power or payload versus size nor is it systematically optimized under strict engineering constraints [10].

To address these deficiencies, this study proposes a systematic design method combining the AHP with Biomimetic Engineering. AHP has been widely validated in numerous complex engineering fields, ranging from the construction sector [11] to operations management [12] and engineering design [13]. It is an effective tool for resolving multi-criteria resource conflicts. Drawing on these precedents, we utilize AHP to shift the rescue vehicle design process from subjective estimation to data-driven decision-making, ensuring that critical functions are prioritized based on mathematical logic rather than intuition.

Regarding the selection of the bionic prototype, we adhere to the principle of environmental isomorphism. The operational environment of post-earthquake rescue is physically characterized by damp, confined spaces and unstructured granular terrain typical of ruins. Survival in such contexts demands a specific set of evolutionary adaptations: powerful excavation capabilities for obstacle clearance and a flexible body structure for navigating restricted tunnels. Based on this rigorous mapping between environmental constraints and functional traits, the mole cricket emerges as the optimal biological template [14]. Its fossorial forelimbs and segmented abdomen provide a pre-validated evolutionary solution to the engineering conflicts between passability and excavation, as well as payload capacity and structural compactness [15].

The remainder of this paper is organized as follows: Section 2 establishes the AHP model to quantitatively analyze the functional requirements of post-earthquake rescue vehicles, determining the core design priorities that guide the subsequent development. Section 3 details the biomimetic design process, justifying the selection of the mole cricket based on environmental isomorphism and illustrating the translation of its biological features into specific mechanical modules. Section 4 conducts a finite element modal analysis to evaluate the dynamic characteristics of the initial design and verifies the structural safety and stability improvements achieved through optimization. Finally, Section 5 summarizes the research conclusions and outlines directions for future work.

2. ANALYSIS OF FUNCTIONAL REQUIREMENTS BASED ON AHP

China is located in the southeast of the Eurasian plate, an area frequently affected by the interaction between the Indian Ocean plate and the Pacific plate. Earthquake disasters occur frequently, mostly in mountainous basins. These disasters are often accompanied by the collapse of roads and bridges, severely hindering rescue equipment from reaching the disaster center. Consequently, post-earthquake rescue scenarios are characterized by high

uncertainty and complexity, requiring rescue vehicles to address a multitude of potential needs ranging from debris clearing to medical transport through various functional combinations. However, due to strict constraints on vehicle spatial structure, payload capacity, and manufacturing costs, it is impractical to integrate all possible functions into a single platform. The critical design challenge, therefore, lies in identifying the most urgent and reasonable configuration among numerous alternatives.

To resolve this multi-criteria decision-making problem, the AHP is utilized to scientifically rationalize design priorities. AHP is a systematic analysis method that combines qualitative analysis with quantitative calculation. Its standard workflow involves four steps: (1) decomposing the complex problem into a hierarchical structure (Target, Criterion, and Factor layers); (2) constructing pairwise comparison matrices using a 1-9 scale to quantify subjective judgments; (3) calculating weight vectors to determine the relative importance of elements; and (4) performing consistency tests to ensure logical validity.

2.1. Decision-Making Logic and Hierarchy Construction

Following this scientific paradigm, we constructed a comprehensive three-level hierarchical model based on the actual post-earthquake rescue needs in China. First, the Target Layer (A) was defined as the overall functional requirement analysis of the post-earthquake rescue vehicle. Second, this goal was decomposed into a Criterion Layer consisting of five core dimensions: Rescue (B), Passing (C), Firefighting (D), Transportation (E), and Treatment (F) requirements. Finally, to ensure operational granularity, these criteria were further substantiated into a Factor Layer comprising specific sub-indicators ranging from traversing collapsed terrain to specific emergency support capabilities. This rigorous qualitative decomposition formed the complete hierarchical analysis structure shown in Figure 1, providing the structural basis for the subsequent quantitative weight calculation.

2.2. Construction of Judgment Matrices for Functional Priorities

To quantify the priorities established in the hierarchical model, we construct pairwise comparison matrices.

Suppose there are n elements (F_1, F_2, \dots, F_n) in a specific layer that need to be compared against a goal from the upper layer. A judgment matrix A is defined as an $n \times n$ matrix:

$$A = (a_{ij})_{n \times n} = \begin{bmatrix} a_{11} & a_{12} & \cdots & a_{1n} \\ a_{21} & a_{22} & \cdots & a_{2n} \\ \vdots & \vdots & \ddots & \vdots \\ a_{n1} & a_{n2} & \cdots & a_{nn} \end{bmatrix}$$

Where a_{ij} represents the relative importance of element i compared to element j . The value of a_{ij} is determined based on the Saaty 1-9 scale definitions shown in Table 1. The matrix satisfies the reciprocal property, meaning that if the importance of element i over j is a_{ij} ,

then the importance of element j over i is $a_{ji} = 1/a_{ij}$, and $a_{ii} = 1$.

Note: Reciprocal scale implies that if the importance of element i to j is a_{ij} , then the importance of j to i is a_{ji} .

Based on this mathematical definition and the specific rescue requirements, all judgment matrices for the Target Layer (A), Criterion Layer, and Factor Layer (B–F) are formulated. The specific values are described in the following equations:

1. Judgment Matrix of the Criterion Layer (Target A):

$$A = \begin{pmatrix} 1 & 1/2 & 5 & 3 & 3 \\ 2 & 1 & 6 & 5 & 5 \\ 1/5 & 1/6 & 1 & 1/2 & 1/3 \\ 1/3 & 1/5 & 2 & 1 & 1 \\ 1/3 & 1/5 & 3 & 1 & 1 \end{pmatrix}$$

2. Judgment Matrices of the Factor Layer (Criteria B-F):

$$B = \begin{pmatrix} 1 & 3 & 5 & 2 \\ 1/3 & 1 & 3 & 1/2 \\ 1/5 & 1/3 & 1 & 1/4 \\ 1/2 & 2 & 4 & 1 \end{pmatrix} \quad C = \begin{pmatrix} 1 & 3 & 2 \\ 1/3 & 1 & 1/2 \\ 1/2 & 2 & 1 \end{pmatrix}$$

$$D = \begin{pmatrix} 1 & 3 & 2 \\ 1/3 & 1 & 1/2 \\ 1/2 & 2 & 1 \end{pmatrix} \quad E = \begin{pmatrix} 1 & 2 & 5 \\ 1/2 & 1 & 2 \\ 1/5 & 1/2 & 1 \end{pmatrix}$$

$$F = \begin{pmatrix} 1 & 1/3 & 1/8 \\ 3 & 1 & 1/3 \\ 8 & 3 & 1 \end{pmatrix}$$

2.3. Single-Level Ranking and Consistency Check

To strictly quantify the functional priorities of the post-earthquake rescue vehicle, we utilize the judgment matrices established in the previous section to calculate the specific weight of each factor. The calculation process uses the Sum-Product Method [16] to derive the eigenvector, which serves as the design priority coefficient for each functional module. The steps are as follows:

1. Normalization of the judgment matrix: Each column vector of the judgment matrix is normalized to eliminate dimensional influence:

$$\bar{a}_{ij} = \frac{a_{ij}}{\sum_{k=1}^n a_{kj}} \quad (i, j = 1, 2, \dots, n) \quad (1)$$

2. Summation by row: The normalized row elements are summed to obtain the preliminary weight vector:

$$\bar{W}_i = \sum_{j=1}^n \bar{a}_{ij} \quad (i = 1, 2, \dots, n) \quad (2)$$

3. Calculation of the weight vector: The vector is normalized again to obtain the final weight vector W, which represents the relative importance of each rescue function:

$$W_i = \frac{\bar{W}_i}{\sum_{j=1}^n \bar{W}_j} \quad (3)$$

$$W = (W_1, W_2, \dots, W_n)^T \quad (4)$$

4. Calculation of the maximum eigenvalue: The maximum eigenvalue λ_{max} is calculated to verify the validity of the weights:

$$\lambda_{max} = \sum_{i=1}^n \frac{(AW)_i}{nW_i} \quad (5)$$

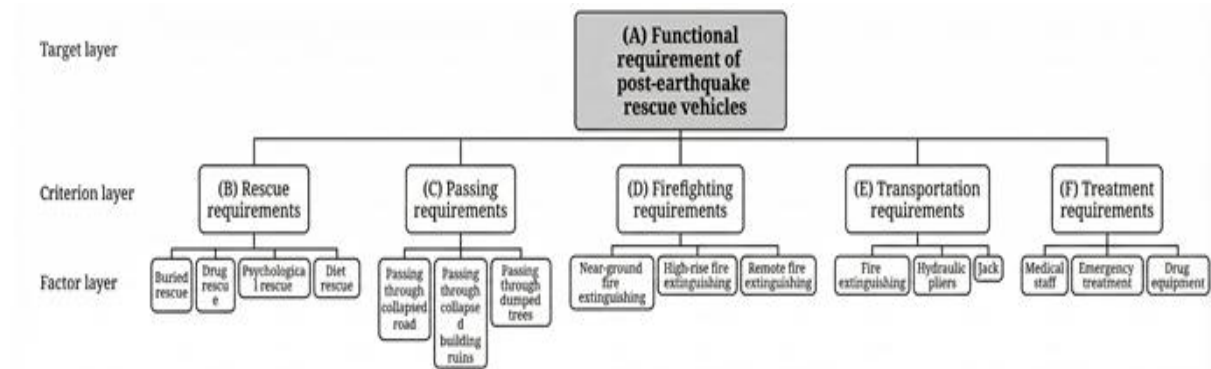


Figure 1. Structure of post-earthquake rescue vehicle demand hierarchy

Table 1. Matrix scale definitions

Scale	Importance	Implication
1	Equally important	The two comparative elements are of equal importance.
3	Slightly important	The former is slightly more important than the latter.
5	Relatively important	The former is more important than the latter.
7	Very important	The former is more important than the latter.
9	Absolutely important	The former is more important than the latter.
2,4,6,8	Between the median value	The importance of the former and the latter

In the engineering design process, subjective judgments regarding complex vehicle functions often contain logical contradictions (e.g., judging "Passing > Rescue" and "Rescue > Fire", but illogically concluding "Fire > Passing"). Therefore, a consistency check is mandatory to ensure the logical validity of the derived weights. The degree of inconsistency is measured by the magnitude of deviation between λ_{max} and n . Define consistency indicators [17]:

$$CI = \frac{\lambda_{max} - n}{n - 1} \tag{6}$$

Where n is the order of the matrix. Generally, if $CI = 0$, the matrix has complete consistency. A larger CI indicates more serious logical inconsistencies in the design judgment. To account for the random deviation in high-order matrices, the Random Consistency Index (RI) is introduced. The RI values corresponding to the matrix order n are listed in Table 2.

Table 2. The first 6th order reciprocal non-negative matrix consistency indicator RI

n	1	2	3	4	5	6	...
RI	0	0	0.58	0.90	1.12	1.24	...

Finally, the Consistency Ratio (CR) is defined as:

$$CR = \frac{CI}{RI} \tag{7}$$

To ensure the scientific rigor of the rescue vehicle design, a $CR < 0.1$ is required. If this condition is met, the judgment matrix is considered to have satisfactory consistency, meaning the calculated weights are logically valid and can be strictly applied to the subsequent biomimetic structural optimization.

2.4. Calculation of Weights and Consistency Verification for Hierarchy Layers

Taking judgment matrix A as an example, it is tested for consistency, and its weight vector and consistency ratio are obtained.

The consistency ratio of all factor layers is shown in Table 3, and it is obvious that the consistency index of all factors is less than 0.1, so we can prove that all judgment matrices have passed the consistency test.

Table 3. Factor layer consistency ratios

Matrix	A	B	C	D	E	F
CR	0.016	0.022	0.0095	0.0078	0.0063	0.0011

2.5. Comprehensive Weight Analysis and Design Strategy

By integrating the weight vectors from all layers, the comprehensive weights of all factors relative to the total target were calculated. The final results are presented in Table 4.

$$\begin{aligned}
 &A = \begin{pmatrix} 1 & 1/2 & 5 & 3 & 3 \\ 2 & 1 & 6 & 5 & 5 \\ 1/5 & 1/6 & 1 & 1/2 & 1/3 \\ 1/3 & 1/5 & 2 & 1 & 1 \\ 1/3 & 1/5 & 3 & 1 & 1 \end{pmatrix} \xrightarrow{\text{Column normalization} \rightarrow \text{processing}} \begin{pmatrix} 0.259 & 0.242 & 0.294 & 0.286 & 0.290 \\ 0.517 & 0.484 & 0.353 & 0.476 & 0.484 \\ 0.052 & 0.081 & 0.059 & 0.048 & 0.032 \\ 0.086 & 0.097 & 0.118 & 0.095 & 0.097 \\ 0.086 & 0.097 & 0.176 & 0.095 & 0.097 \end{pmatrix} \\
 &\xrightarrow{\text{Sum by row}} \begin{pmatrix} 1.311 \\ 2.314 \\ 0.272 \\ 0.493 \\ 0.551 \end{pmatrix} \xrightarrow{\text{Column normalization processing}} \begin{pmatrix} 0.274 \\ 0.463 \\ 0.054 \\ 0.099 \\ 0.110 \end{pmatrix} = \omega \quad \text{Then} \quad A\omega = \begin{pmatrix} 1.403 \\ 2.380 \\ 0.272 \\ 0.501 \\ 0.555 \end{pmatrix} \\
 &\lambda_{max} = \frac{1}{5} \left(\frac{1.403}{0.274} + \frac{2.380}{0.463} + \frac{0.272}{0.054} + \frac{0.501}{0.099} + \frac{0.555}{0.110} \right) = 5.081
 \end{aligned}$$

Table 4. Results of the synthesis weights

Criterion layer and its weight	Factor level		Comprehensive weight	Integrated ranking
	Factor	Weight		
(A)Rescue requirements (0.274)	B1 Buried rescue	0.475	0.130	3
	B2 Drug rescue	0.170	0.047	8
	B3 Psychological rescue	0.079	0.022	12
	B4 Diet rescue	0.276	0.076	5
(B)Passing requirements (0.463)	C1 Passing through the collapsed road	0.541	0.250	1
	C2 Passing through the collapsed building ruins	0.169	0.078	4
	C3 Passing through dumped trees	0.290	0.134	2
(C)Firefighting requirements (0.054)	D1 Near-ground fire extinguishing	0.539	0.029	9
	D2 High-rise fire extinguishing	0.164	0.009	16
	D3 Remote fire extinguishing	0.297	0.016	13
(D)Transportation requirements (0.099)	E1 Fire extinguisher	0.595	0.059	7
	E2 Hydraulic pliers	0.277	0.027	10
	E3 Jack	0.129	0.013	14
(E)Treatment requirements (0.110)	F1 Medical staff	0.082	0.009	15
	F2 Emergency treatment	0.236	0.026	11
	F3 Drug equipment	0.682	0.075	6

Analysis of Results: The quantitative data in Table 4 reveals a distinct functional hierarchy. At the criterion layer, "Passing Requirements" (0.463) and "Rescue Requirements" (0.274) are the dominant factors, cumulatively accounting for over 73% of the total weight. This data distribution indicates that in the context of Chinese post-earthquake rescue, "mobility" and "active excavation" are the core capabilities, while "Treatment" (0.110), "Transportation" (0.099), and "Firefighting" (0.054) act as secondary support systems. This reflects the engineering reality that reaching the disaster site and clearing ruins are prerequisites for all other rescue operations.

These quantitative AHP results serve as strict engineering guidelines for the subsequent conceptual design. The calculated functional priorities dictate the following structural layout and morphological strategies:

1. Adaptive High-Passability Chassis: Driven by the dominant "Passing" weight (0.463), the chassis architecture prioritizes geometric flexibility over speed. The strategy requires a reconfigurable suspension system capable of handling vertical height differences in ruins. This points towards a locomotion configuration that combines articulated support with high-friction propulsion to ensure stability on complex terrains.
2. Integrated Dual-End Excavation: With "Buried Rescue" (0.130) as a critical factor, the vehicle serves as an active working platform. The design must integrate dual-end actuating mechanisms: a front device for rapid obstacle pushing/clearing and a heavy-duty arm for deep debris removal, enabling multidimensional "pushing, digging, and grabbing" capabilities.
3. Variable-Volume Body Architecture: To reconcile the conflict between "Transportation capacity" and "Mobility," a static cargo space is suboptimal. The strategy adopts a telescopic or segmented body structure. This allows the vehicle to expand for maximum payload (supplies) and contract to a compact form for traversing narrow spaces.
4. Functional Surface Engineering: Addressing the muddy disaster environment, the exterior requires low-adhesion functional coatings. This ensures friction reduction during movement and maintains visual recognizability for psychological rescue, reducing maintenance needs.

3. KEY POINTS OF BIONIC MODELING DESIGN BASED ON MOLE CRICKET CHARACTERISTICS

The quantitative analysis in the preceding chapter underscored the critical demand for a vehicle combining high trafficability, active excavation, and flexible loading capabilities. However, current post-earthquake rescue equipment is mostly modified from single-function engineering machinery, failing to provide sufficient reference for such a highly integrated layout. Consequently, we turned our gaze to nature. Life forms in nature are full of examples of "perfect design" after millions of years of natural evolution, which is a huge treasure trove of bionic design knowledge for designers. When designing automotive products, we adopt the bionic design concept, combined with the characteristics of natural fantasy creatures, referring to the structure, function, form, and color of natural creatures, and supplemented by modern design thinking and methods, we can create a combination of nature and modernity. The beautiful vehicle shape can stand out in the modern public aesthetics. The bionic design can also guide the overall structural design and functional design of the vehicle. Therefore, this study will focus on those organisms that can survive in an environment similar to the one left behind after an earthquake. Based on this environmental similarity, the Mole Cricket was identified as the best prototype.

To translate this biological inspiration into a mechanical reality, we adopted a systematic bionic design approach. This involves deconstructing the mole cricket's biological advantages specifically its fossorial adaptability and structural robustness and mapping them to the vehicle's functional modules. So in this specific design implementation, the function, shape, color, and structure of the mole cricket are comprehensively extracted. Notably, guided by the previous weight analysis, the design prioritizes the structural evolution of the excavation and locomotion systems. The physical characteristics, such as its robust muscular sensation and streamlined contours, are abstractly evolved and applied to the vehicle's functional requirements, as shown in Figure 2.

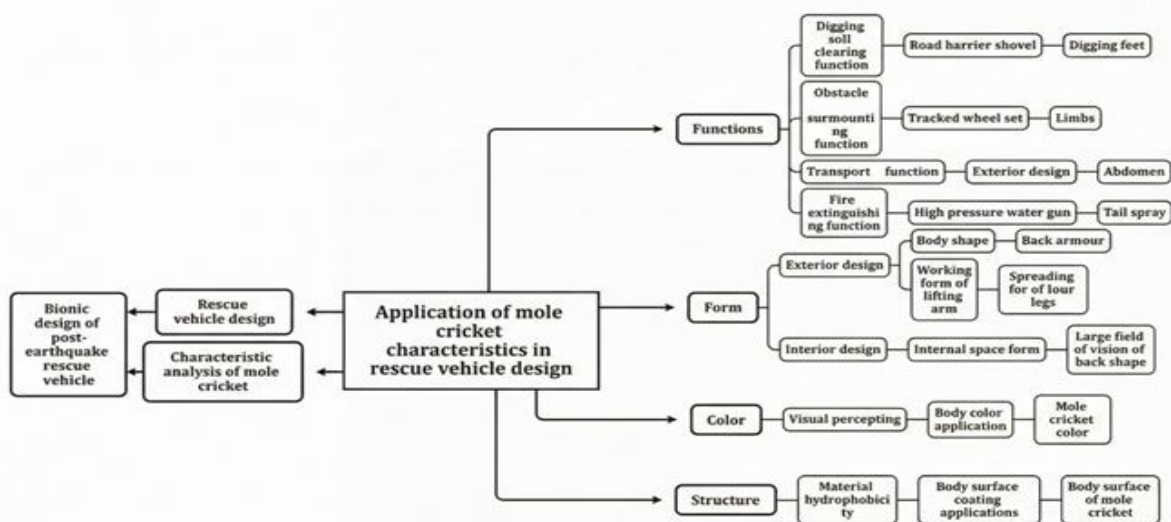


Figure 2. The specific application of the characteristics of the mole cricket in the design of the rescue vehicle after the earthquake

3.1. Analysis of the Overall Shape Design of the Mole Cricket

To translate the biological morphology of the mole cricket into a mechanical rescue vehicle, we employed a "block abstraction and surface evolution" method. Crucially, this morphological evolution was not arbitrary; it was strategically aligned with the functional hierarchy established by the AHP analysis in Section 2. The dominance of "Passing" and "Rescue" weights dictated that the evolution process must prioritize chassis stability and the integration of excavation structures over mere aesthetic mimicry. As illustrated in Figure 3, the complex biological form was decomposed into 10 key characteristic surfaces and evolved through the following specific steps:

1. Step 1: Geometric Abstraction (Figure 3(a) to Figure 3(b)): Figure 3(a) shows the original biological prototype. In Figure 3(b), we performed the initial geometric abstraction. The organic, complex biological outlines were simplified into basic geometric blocks. Specifically, the head and thorax (Block 1) were abstracted into a wedge shape. This design is not only visually dynamic but also functional for a ground vehicle, assisting in deflecting falling debris and reducing frontal impact area in narrow ruins.
2. Step 2: Mechanical Sharpening (Figure 3(b) to Figure 3(c)): To embody the "robustness" and "stability" required for a rescue vehicle, we sharpened the geometry. The original rounded blocks were transformed into angular, diamond-cut surfaces. Surface 3 evolved from a trapezoid to a diamond shape to visually lower the center of gravity, enhancing the perception of chassis stability required for off-road operations.
3. Step 3: Functional Integration (Figure 3(c) to Figure 3(d)): This phase focused on integrating rescue functions. Surface 1 was further sharpened to create a streamlined profile that prevents the vehicle from getting snagged on rebar or branches in debris fields. Crucially, Surface 5 was elongated, evolving from the biological

wing structure into the mechanical linkage of the rear excavation arm, directly responding to the high-priority "Rescue" requirement. Surfaces 8, 9, and 10 were arranged in a ladder formation to form the protective shell of the telescopic tail warehouse.

4. Step 4: Hierarchical Refinement and Fusion (Figure 3(e) to Figure 3(f)): In Figure 3(e), Surface 1 was refined into a faceted structure to give the front cabin a protective, armored appearance. Surface 4 was elevated to improve the driver's field of view over obstacles. Finally, in Figure 3(f), surfaces 1, 3, and 4 were merged into a cohesive unibody cabin, and the end of Surface 5 was detailed into the excavation hook. This completed the evolution from an insect to a high-mobility rescue platform.

3.2. Engineering Design of the Bionic Front Obstacle-Clearing Bucket

By extracting the characteristics of the mole cricket limbs, it can be seen that the body structure of the mole cricket, especially the front claws, has evolved typical biological characteristics that can adapt to the soil environment. To translate this biological advantage into engineering feasibility, we designed the front working device as a hydraulic multi-joint actuation system.

As shown in Figure 4, structurally, the bucket adopts a double-opening claw configuration mimicking the mole cricket's "tibial claws." Unlike traditional static buckets, this design features independent hydraulic cylinders controlling the opening and closing angles. This grants the mechanism two distinct operational modes.

The first mode is the bulldozer mode. When the bucket is closed, it forms a wedge-shaped shield (similar to the digging posture of an insect), which can efficiently push aside heavy obstacles such as stones and concrete blocks. The second mode is the grasping mode. When the bucket is opened, the serrated edges (imitating the joints of a living organism) engage to grasp and lift the debris.

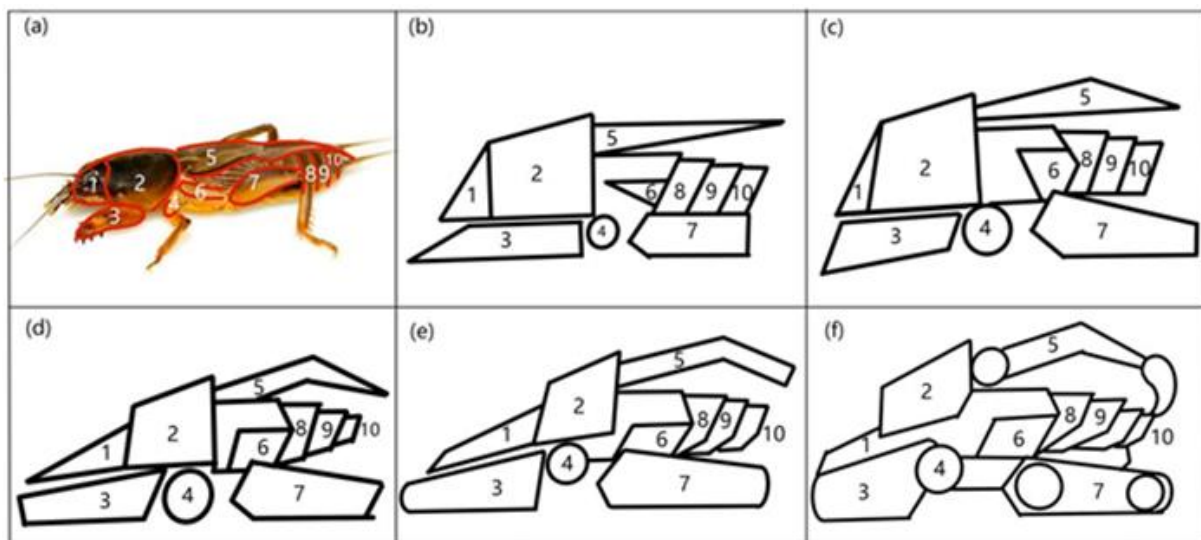


Figure 3. Schematic diagram of the contour line evolution of rescue vehicle based on the morphological characteristics of the mole cricket

As shown in Figure 5, this biological feature can be transformed into an arm with 3 degrees of freedom for digging, enabling it to perform complex spatial operations in narrow ruins.

3.3. Biomimetic Design of the Tail Excavation Arm

The challenge of the rear excavation module lies in balancing "reach capability" with "compact storage." Nature provides an optimal solution in the mole cricket's wing folding mechanism. While the insect's wings are large when deployed, they fold compactly along the dorsal axis when at rest. Drawing from this biological principle, we designed the tail excavation arm as a multi-stage folding boom system (as shown in Figure 6). Drawing inspiration from the folding mechanism of the mole cricket's wings, the tail excavation arm is designed to alternate seamlessly between a compact transport state and an active operational state. In the transport mode, the arm folds flat against the vehicle's dorsal surface, mimicking the insect's "sword-shaped" wing contour; this configuration not only minimizes the vertical profile to prevent collisions with obstacles but also effectively lowers the center of gravity for enhanced stability. Conversely, for active operation (as shown in Figure 7), the system deploys via a series linkage mechanism driven by high-power hydraulic cylinders. Here, the bionic "wing" morphology is engineered into reinforced structural booms, which provide the necessary flexural strength for heavy-duty digging and enable a wide operational radius to clear debris without repositioning the chassis. This dual-mode functionality demonstrates how the bionic wing morphology successfully translates into a

highly space-efficient and mechanically robust engineering structure.

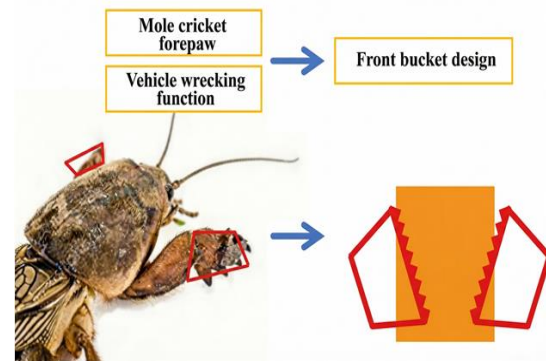
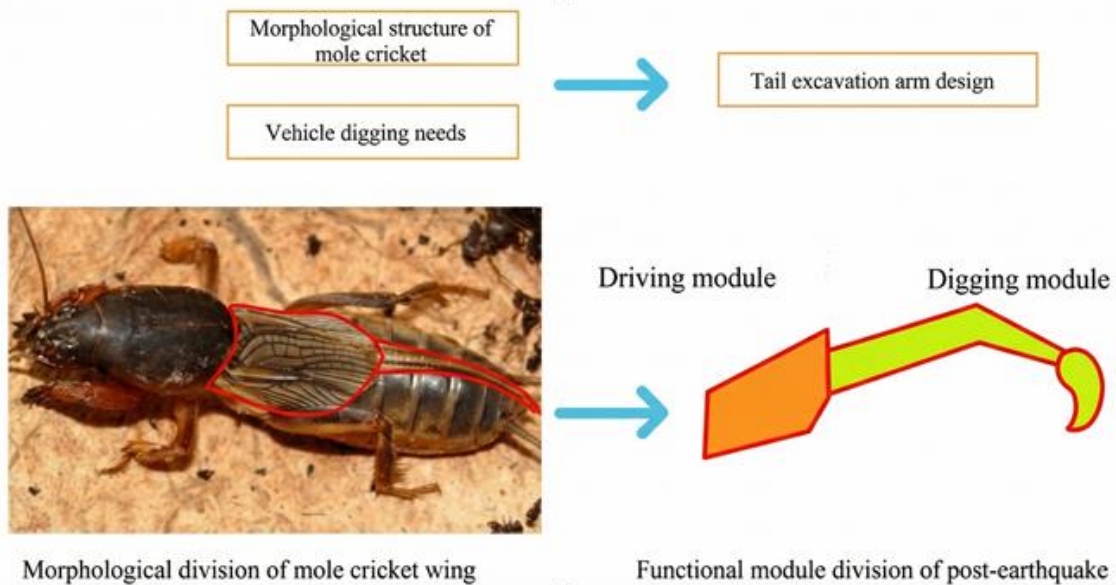


Figure 4. Illustration of a simulated front digging bucket of a caddisnot digging foot



Figure 5. Rescue vehicle double digging grapple display



Morphological division of mole cricket wing

Functional module division of post-earthquake

Figure 6. Excavation of the large arm bionic fly wings in the tail of the rescue vehicle



Figure 7. Rescue vehicle tail gouging arm display

3.4. Bionic Design of Contractible Tailstock

The tail of the post-earthquake rescue vehicle extracts the segmented morphological features of the mole cricket abdomen, as shown in Figure 8, and the characteristic curve is abstracted into a telescopic nested structure. The rescue vehicles require a large number of items to carry, and it is necessary to reasonably allocate the carrying space. The bionic multi-stage sliding design of the tail can be

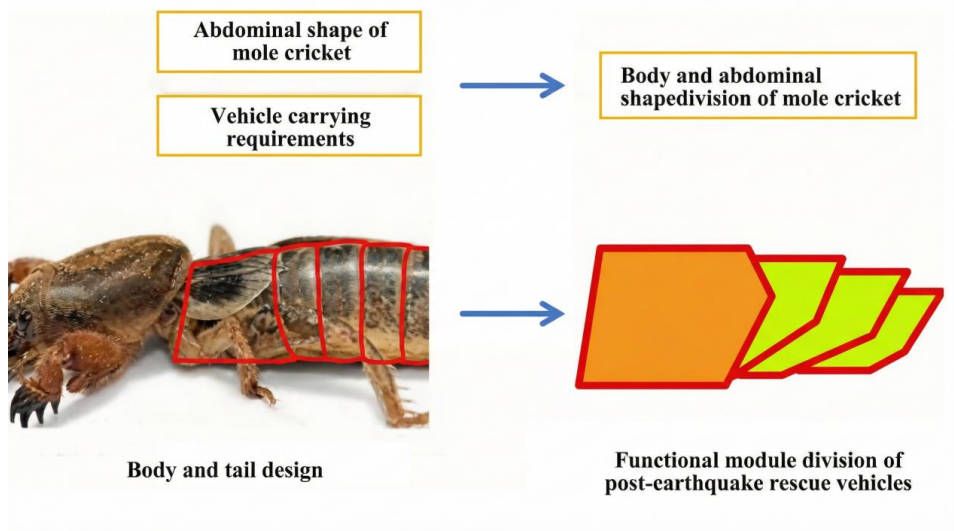


Figure 8. The shape of the abdomen of the vehicle body and the tail of the bionic moth is indicated



Figure 9. Rescue truck retractable tailpipe design display

longitudinally extended or retracted via electric linear actuators according to the carrying capacity. This allows the effective volume of the tail warehouse to be adjusted according to specific needs. Crucially, when traversing complex terrain, the retraction of the tail centralizes the vehicle's mass and significantly increases the departure angle. This structure prevents tail scraping and improves the obstacle-surmounting ability of the vehicle, as shown in Figure 9.

3.5. Biomimetic Functional Structure of the Chassis

In order to meet the needs of the rescue vehicle to cross the road and pass through the obstacle section after the earthquake, an adaptive locomotion system is required. In the process of designing the chassis, the bionic mole cricket limb is shown in Figure 10, and the articulated quad-track configuration is adopted. Each crawler module is mounted on an independent swing arm controlled by a separate hydraulic support system. This active suspension design can complete the action of lifting, lowering, and leveling the body. By independently adjusting the height of each track, the system can maximize ground clearance when crossing ruins, so as to improve the obstacle-crossing ability and greatly meet the trafficability requirements of the rescue vehicle, as shown in Figure 11.

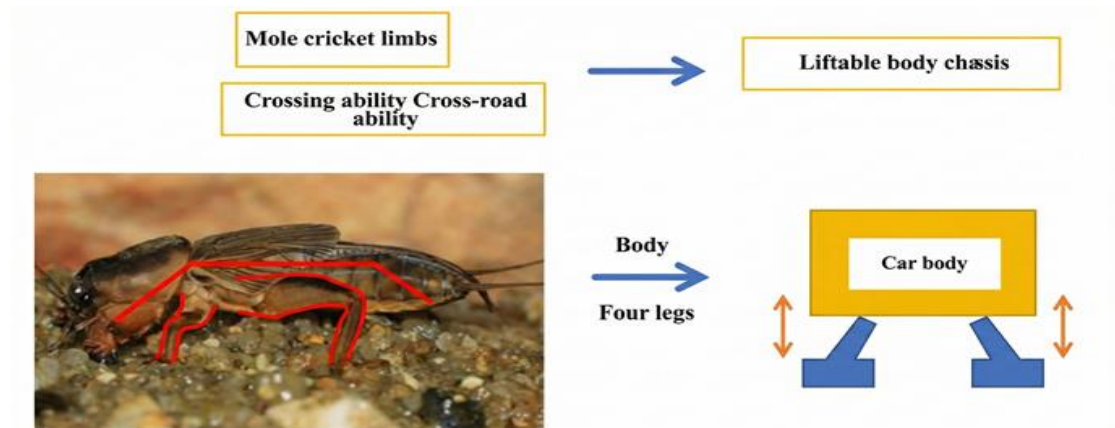


Figure 10. Bionic mole cricket foot of vehicle underframe display



Figure 11. Rescue vehicle can lift wheelset details

3.6. Biomimetic Application of Hydrophobic Coating for Functional Surface

Post-earthquake environments are often characterized by high humidity and muddy terrain, which can cause soil adhesion to the vehicle body, increasing drag and obscuring sensors. To address this, we propose a functional coating inspired by the hydrophobic cuticle of the mole cricket.

Existing biological studies have confirmed that the mole cricket's exoskeleton is covered with a micro-nano structure of short bristles, which creates a composite interface that traps air [18]. According to the Cassie-Baxter model, this structure significantly reduces the contact area between water/soil and the body surface, resulting in a high contact angle that repels mud and water. Drawing from this validated biological mechanism, we designed the vehicle's exterior coating to mimic this micro-texture. By preventing mud accumulation on the chassis and tracks, the coating reduces the vehicle's moving load and energy consumption. The hydrophobic property allows contaminants to roll off easily (Lotus Effect), ensuring that the vehicle's "Rescue Orange" color remains visible for psychological relief and that optical sensors remain unobstructed without frequent manual cleaning.

3.7. Bionic Modeling Design of Post-Earthquake Rescue Vehicles

Many wonderful biological characteristics in nature have been feature extracted and performed artistic processing by the designer, and applied to vehicle design in combination with the principle of bionics, so as to design a powerful,

novel and convenient driving post-earthquake rescue vehicle. The rescue vehicle fully extracts the body characteristics and structure of insect mole crickets for bionic redesign, so that the rescue vehicle has strong obstacle clearance, excavation, transportation, obstacle crossing and fire extinguishing capabilities. The front digging foot with the most limb characteristics of mole cricket is designed by using the bionic principle to design a rescue vehicle with double obstacle clearance front digging bucket with mole cricket digging foot shape and motion characteristics. The characteristics of the 'sword' wings of the mole cricket are divided into blocks, and the overall shape outline of the cab and the function of excavating the arm structure are extended so that the rescue vehicle has a broad and clear vision in the rescue process; by using the principle of bionic abstract evolution, the laminated abdomen of the mole cricket is used in the design of the rear part of the rescue vehicle, so that the rear storage warehouse has contraction and extension, and the rescue materials are carried as much as possible. The characteristics of supporting the body of mole cricket limbs away from the ground friction are applied to the chassis design of the post-earthquake rescue vehicles, so that the rescue vehicle has strong trafficability and mobility. The overall shape of the rescue vehicle is divided into blocks by the overall characteristics of the mole cricket body, and then the overall shape outline of the rescue vehicle is gradually formed through the abstract evolution principle, as shown in Figure 13, which is the design sketch of the rescue vehicle. Based on the sketch, the overall effect map of the post-earthquake rescue vehicle is obtained through modeling and rendering software processing, as shown in Figure 14.



Figure 12. Surface hydrophobic application of the mole cricket



Figure 13. Sketch of the design of the rescue vehicle after the earthquake



Figure 14. Post-earthquake rescue vehicle design effect display

4. DESIGN OPTIMIZATION

4.1. Modal Analysis and Weakness Identification

Modal analysis technology is widely used in automobile structure design to effectively analyze structural system vibration [19]. In this section, UG12 software is used to perform modal analysis. Theoretically, the vehicle has infinite-order modes; however, since high-order modes have little effect on the overall dynamic analysis [20], we calculated the first six vibration modes to identify maximum deformation positions. The displacement nephograms (Figure 15-20) visualize these modes.

The specific modal results are listed in Table 5. A critical analysis of these data reveals specific structural vulnerabilities.

The first-order natural frequency is 9.03 Hz, with subsequent frequencies clustered between 9-13 Hz. From an engineering perspective, this frequency range is relatively low and dangerously close to the typical excitation frequencies of road roughness or low-speed diesel engines. This creates a significant risk of resonance, which could lead to structural fatigue or control instability during rescue operations. As shown in the "Deformation position" column,

the maximum deformation consistently occurs in the Tail Warehouse for the first three modes. This indicates that the tail's large-area thin-plate structure lacks sufficient local stiffness. Although the maximum stress (1.309 MPa) is low, the excessive flexibility in the tail could cause jamming of the telescopic mechanism or loosening of cargo during movement.

Therefore, the tail warehouse and crawler connection are identified as the "weak links" requiring optimization.

Table 5. Modal analysis results

Order	Natural frequency (Hz)	Maximum displacement(mm)	Stress (MPa)	Deformation position
1	9.031 76	0.1001	0.502	Tail warehouse
2	9.837 23	0.154	0.346	Tail warehouse
3	10.409 9	0.124	0.485	Tail warehouse
4	11.691 3	0.145	1.247	crawler
5	11.692 4	0.145	1.246	crawler
6	13.357 3	0.1145	1.309	crawler

3_sim1 : Copy of Copy of Solution 1
Subcase - Eigenvalue Method 1, 1, 9.03176Hz
: 0.0000, : 0.1001, = mm
: -

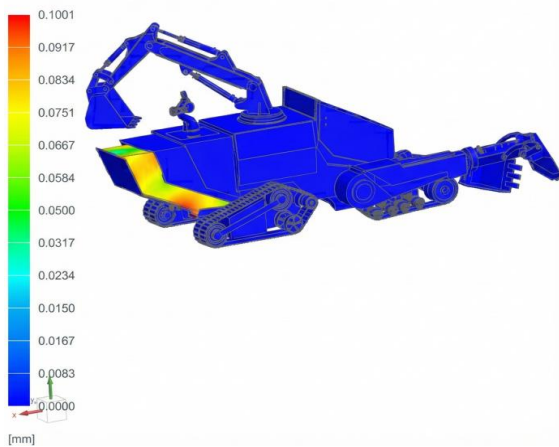


Figure 15. Overall first-order displacement cloud diagram

3_sim1 : Copy of Copy of Solution 1
Subcase - Eigenvalue Method 1, 2, 9.83723Hz
: 0.000, : 0.154, = mm
: -

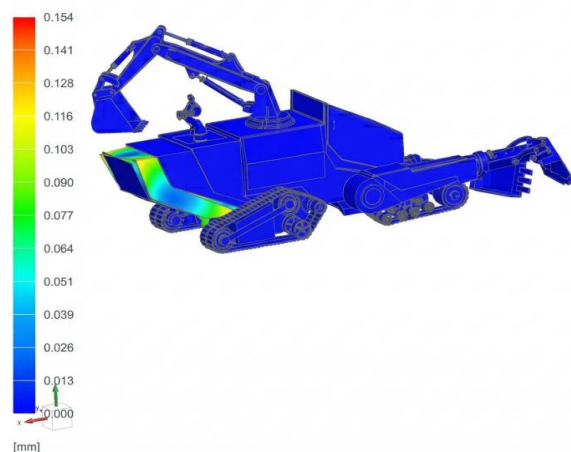


Figure 16. Overall second-order displacement cloud diagram

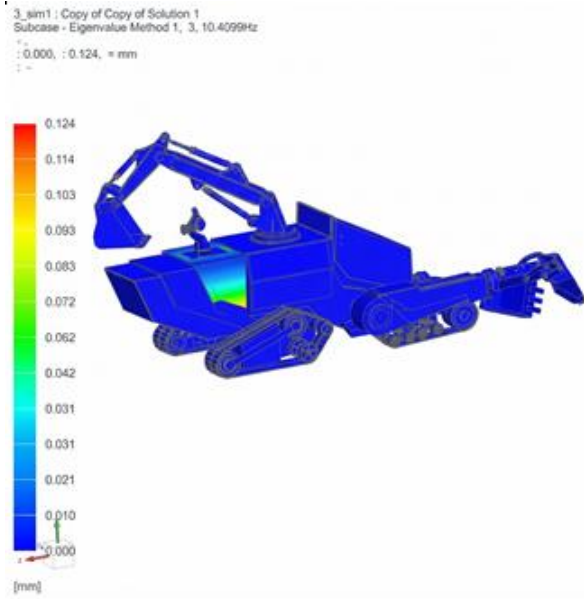


Figure 17. Overall third-order displacement cloud diagram

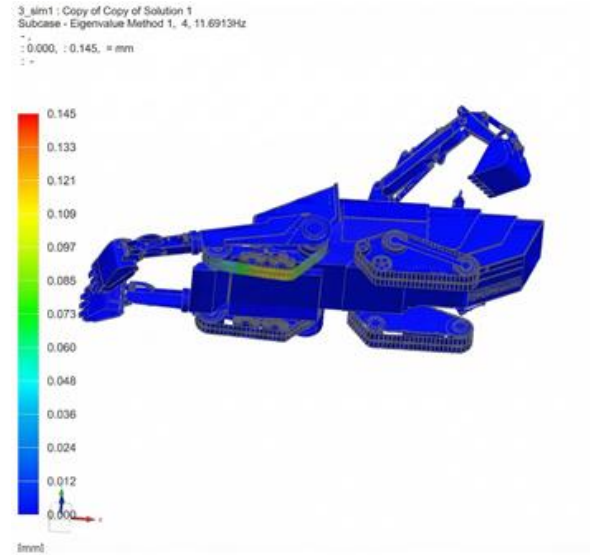


Figure 18. Overall fourth-order displacement cloud diagram

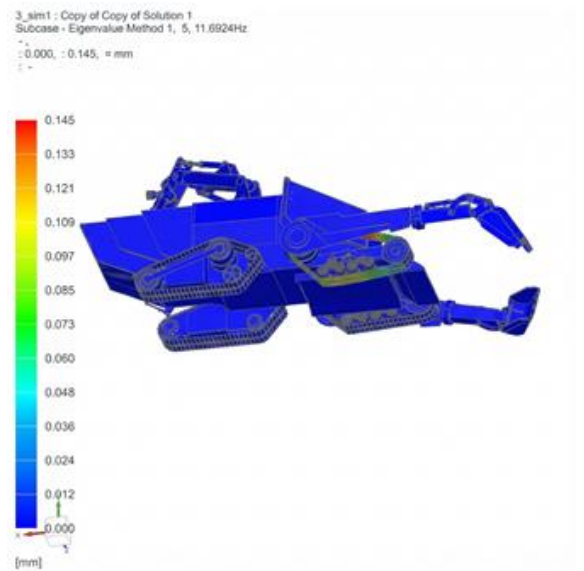


Figure 19. Overall fifth-order displacement cloud diagram

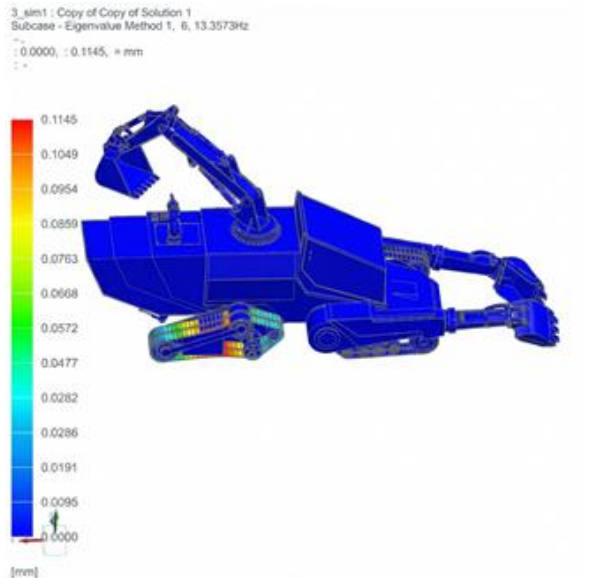


Figure 20. Overall sixth-order displacement cloud diagram

The optimized results are presented in Table 6. Comparing Table 6 with Table 5 reveals significant engineering improvements.

The fundamental frequency increased from 9.03 Hz to 13.93 Hz (a 54.27% increase). Crucially, this shift moves the vehicle's natural frequency away from the sensitive low-frequency excitation zone (typically <10 Hz for rough terrain), significantly reducing the probability of resonance and enhancing dynamic stability. The maximum displacement shifted from the main "Tail Warehouse" structure to the localized "Tool Warehouse Door." This suggests that the overall structural rigidity of the main body has been successfully reinforced, forcing vibration energy to dissipate into smaller, non-critical components. The maximum stress after optimization is 1.892 MPa. Compared to the allowable yield strength of the material, the safety factor is extremely high. This confirms that the vehicle not

only meets the stiffness requirements but also possesses a substantial safety margin against yield failure.

Table 6. Results of the modal analysis after optimization

Order	Natural frequency (Hz)	Maximum displacement(mm)	Stress (MPa)	Deformation position
1	13.933 5	0.414	1.522	Tool warehouse door
2	13.934 4	0.413	1.459	Tool warehouse door
3	13.934 6	0.410	1.385	Tool warehouse door
4	13.955 9	0.410	0.995	Tool warehouse door
5	17.085 2	0.186	0.610	Tool warehouse door
6	18.939 5	0.385	1.892	Tool warehouse door

To interpret the practical significance of these simulation results, we benchmarked the data against standard engineering material limits. The rescue vehicle structure is

constructed primarily using Q345 Structural Steel, which has a standard Yield Strength (σ_s) of 355 MPa.

Stress Validation: The simulation results in Table 6 show a maximum Von Mises stress of $\sigma_{max} = 1.892$ MPa after optimization. Comparing this to the material standard:

$$\sigma_{max} (1.892 \text{ MPa}) \ll \sigma_{allowable} (355 \text{ MPa})$$

The calculated Safety Factor (S) is:

$$S = \frac{\sigma_{allowable}}{\sigma_{max}} \approx 187$$

This extremely high safety margin confirms that the optimized bionic structure is robust. It operates deep within the linear elastic region, ensuring that no plastic deformation or yield failure will occur even under dynamic vibration loads significantly higher than the simulated conditions.

Displacement Evaluation: The maximum displacement is recorded as 0.414 mm at the "Tool Warehouse Door." Considering the vehicle's overall length (approx. 4000-5000 mm), this relative deformation is less than 0.01%. From an engineering perspective, this magnitude of deformation is negligible. It validates that the thickened plates and added stiffeners have successfully provided sufficient structural stiffness, preventing any excessive flexing that could jam the telescopic tail mechanism or affect chassis stability.

By comparing and calculating the frequency results of the six-order modal displacement diagram before and after the optimization of the rescue vehicle, the optimization rate can be obtained, as shown in Table 7.

Table 7. Optimization rates

Order	Original natural frequency (Hz)	Optimized natural frequency (Hz)	Optimization rate
1	9.031 76	13.933 5	54.27%
2	9.837 23	13.934 4	41.65%
3	10.409 9	13.934 6	33.86%
4	11.691 3	13.955 9	12.20%
5	11.692 4	17.085 2	46.12%
6	13.357 3	18.939 5	41.80%

As quantified in Table 7, the optimization yielded substantial improvements, with the first-order natural frequency increasing by 54.27% (from 9.03 Hz to 13.93 Hz). From a practical engineering perspective, these numerical increases translate into critical performance enhancements, primarily centering on resonance avoidance and structural durability. The original fundamental frequency (9.03 Hz) was dangerously close to the typical external excitation frequencies of rough post-earthquake terrain (often <10 Hz) and engine idling. By raising the fundamental frequency to 13.93 Hz, the optimized design effectively shifts the structure's resonance point away from these external excitation zones, significantly reducing the likelihood of sympathetic vibration during rescue operations. Furthermore, this increase in frequency corresponds to a significant enhancement in global stiffness; in dynamic environments, a stiffer structure experiences lower deformation amplitudes under cyclic loading, which directly contributes to improved fatigue resistance and extends the vehicle's service life in harsh conditions. Finally, for a

vehicle equipped with a biomimetic excavation arm, this structural rigidity is vital as it ensures the chassis provides a stable, non-compliant base during digging and lifting operations, thereby improving the control accuracy of the bionic mechanisms. In conclusion, the optimization successfully transformed the vehicle from a vibration-prone structure into a rigid, durable platform that fully meets the dynamic requirements of post-earthquake rescue.

5. CONCLUSION

This study successfully established a systematic design framework for post-earthquake rescue vehicles by integrating quantitative decision-making with biomimetic engineering. By bridging the gap between theoretical requirements and physical implementation, we proposed a novel vehicle morphology that balances high trafficability with active rescue capabilities.

Regarding the quantitative identification of design priorities, the Analytic Hierarchy Process (AHP) was utilized to clarify the complex functional requirements of rescue operations. The analysis quantified that "Passing Requirements" (Weight: 0.463) and "Rescue Requirements" (Weight: 0.274) are the dominant design constraints. This quantitative hierarchy provided the critical engineering directive to prioritize the chassis trafficability and active excavation capabilities over auxiliary functions. Consequently, this data-driven prioritization fundamentally shifted the design focus from a "general-purpose transport vehicle" to a "specialized high-mobility working platform."

Subsequently, the biomimetic structural realization was strictly guided by these AHP directives. The mole cricket was identified and utilized as the optimal prototype, and the study successfully translated the insect's biological advantages into mechanical solutions through a rigorous feature mapping process. Specifically, the fossorial forelimbs were engineered into a high-power front obstacle-clearing bucket and rear excavation arm to satisfy the rescue priority, while the segmented abdomen was evolved into a variable-volume telescopic tail warehouse. This morphological evolution realized a critical balance between functional integration and spatial efficiency, validating the feasibility of the bio-inspired layout.

Furthermore, the verification of performance optimization confirmed the design's validity. The modal analysis and subsequent optimization yielded significant quantitative improvements in structural dynamics. The optimization strategy focusing on stiffening the tail and chassis through plate thickening and rib reinforcement resulted in an increase of the first-order natural frequency from 9.03 Hz to 13.93 Hz, representing a 54.27% improvement. This substantial shift effectively moves the vehicle's resonance point away from the low-frequency excitation zone of rough terrain, ensuring dynamic stability and proving the structural robustness of the design.

Finally, while this study validated the conceptual feasibility and dynamic stiffness of the proposed vehicle, we acknowledge several limitations that define the roadmap for future research. The first limitation concerns mechanical reliability; while the current simulation focused on resonance prevention, the static load-bearing capacity under extreme payload conditions and the long-term fatigue life of the telescopic mechanisms have not yet been quantified.

Future work will involve comprehensive Static Structural Analysis and Fatigue Analysis. The second area addresses kinematic control, as this paper established the structural morphology but did not cover the motion control strategies required for the complex articulated crawler chassis. Subsequent research will focus on kinematic simulation to develop adaptive gait planning algorithms. The third aspect involves physical validation, as the current work relies on numerical simulation. The efficacy of the hydrophobic coating and the actual maneuverability remain to be tested physically. Therefore, the next phase aims to manufacture a scaled physical prototype to conduct field testing in simulated disaster environments, providing empirical data to calibrate the models and verify performance.

Funding Statement

This project was funded by Major Science and Technology Project of Yunnan Province (202402AE090027), Liberal Arts Program of Southwest Forestry University (11050218).

Data Availability Statement

All data generated or analysed during this study are included in this article.

Conflict of Interest

The authors declare that they have no competing interests.

References

- [1] S. Dong, Y. Zhang, "Research Status and Development Suggestions of High Mobility Multi-Functional Emergency Rescue Equipment", *IOP Conference Series: Earth and Environmental Science*, Vol. 252, 2019, pp. 032153. <https://doi.org/10.1088/1755-1315/252/3/032153>.
- [2] X. Zang, Y. Liu, Z. Lin, C. Zhang, S. Iqbal, "Two multi-linked rescue robots: design, construction and field tests", *Journal of Advanced Mechanical Design, Systems, and Manufacturing*, Vol. 10, No. 6, 2016, pp. 16-00176. <https://doi.org/10.1299/jamdsm.2016jamdsm0089>.
- [3] J. Hou, Z. Xue, Y. Liang, Y. Sun, Y. Zhao, Q. Chen, "Self-Configurable Centipede-Inspired Rescue Robot", *Applied Sciences*, Vol. 14, No. 6, 2024, pp. 2331. <https://doi.org/10.3390/app14062331>.
- [4] G. Chen, K.-C. Wang, L. Wu, S.-Y. Zhan, "A Novel Design of a Small Adaptive Bionic Obstacle-crossing Vehicle", *Sensors and Materials*, Vol. 36, No. 6, 2024, pp. 2351-2370. <https://doi.org/10.18494/SAM4879>.
- [5] M. Jiang, W. Deng, H. Lin, "Sustainability through Biomimicry: A Comprehensive Review of Bionic Design Applications", *Biomimetics*, Vol. 9, No. 9, 2024, pp. 507. <https://doi.org/10.3390/biomimetics9090507>.
- [6] S. Wang, J. Li, X. Gao, B. H. Yan, "Conceptual Design of Four Rotors Flying Car Based on Bionics", 5th International Conference on Mechatronics, Materials, Chemistry and Computer Engineering (ICMMCCE 2017), 2017, Article ID 166. <https://doi.org/10.2991/icmmcce-17.2017.166>.
- [7] T. Aguilar-Planet, E. Peralta, "Innovation Inspired by Nature: Applications of Biomimicry in Engineering Design", *Biomimetics*, Vol. 9, No. 9, 2024, pp. 523. <https://doi.org/10.3390/biomimetics9090523>.
- [8] N. Klyusov, N. Garin, S. Usenyuk-Kravchuk, E. Vasilieva, K. Ustinov, "A Biomorphic Approach to Designing Special-Purpose Vehicles for Arctic Conditions", *Biomimetics*, Vol. 8, No. 4, 2023, pp. 360. <https://doi.org/10.3390/biomimetics8040360>.
- [9] T. Estêvão, M. Araújo, "Territorial and Industrial Challenges in the Automotive and Aeronautic Sectors: Report and conclusions on industrial and regional strategic orientations and challenges". SCAIRA Project, Interreg Sudoe, 2024.
- [10] P. Bao, L. Shi, L. Duan, et al., "A Review: From Aquatic Lives Locomotion to Bio-inspired Robot Mechanical Designations", *Journal of Bionic Engineering*, Vol. 20, 2023, pp. 2487-2511. <https://doi.org/10.1007/s42235-023-00421-2>.
- [11] A. Darko, A. P. C. Chan, E. Effah, E. K. Owusu, E. Pärn, D. J. Edwards, "Review of application of analytic hierarchy process (AHP) in construction", *International Journal of Construction Management*, Vol. 19, No. 5, 2019, pp. 436-452. <https://doi.org/10.1080/15623599.2018.1452098>.
- [12] S. Wang, J. Fan, Y. Liu, "Simulation Analysis of Frog-Inspired Take-Off Performance Based on Different Structural Models", *Biomimetics*, Vol. 9, No. 3, 2024, pp. 168. <https://doi.org/10.3390/biomimetics9030168>.
- [13] E. Triantaphyllou, S. H. Mann, "Using the analytic hierarchy process for decision making in engineering applications: Some challenges", *The International Journal of Industrial Engineering: Theory, Applications and Practice*, Vol. 2, No. 1, 1995, pp. 35-44.
- [14] Y. Zhang, J. Cao, Q. Wang, et al., "Motion Characteristics of the Appendages of Mole Crickets during Burrowing", *Journal of Bionic Engineering*, Vol. 16, No. 2, 2019, pp. 319-327. <https://doi.org/10.1007/s42235-019-0027-2>.
- [15] C. Yang, Y. Li, K. Huang, J. Wang, M. Zhou, "Bionic Study of Hydraulic Excavator Attachment", *Applied and Natural Science*, Vol. 5, No. 2, 2013, pp. 374-80. <https://doi.org/10.3968/j.ans.1715787020120502.1853>.
- [16] L. Xu, B. Cao, X. Wei, B. Li, J. Su, S. Ning, J. Zhao, "Using analytic hierarchy process to evaluate deep learning for infrared target recognition", *Multimedia Tools and Applications*, Vol. 83, No. 36, 2024, pp. 86229-86232. <https://doi.org/10.1007/s11042-024-20373-x>.
- [17] S. Lin, H. Sun, G. Yan, K. Que, S. Xu, Z. Tang, G. Wang, J. Li, "Structural Design and Analysis of Bionic Shovel Based on the Geometry of Mole Cricket Forefoot", *Agriculture*, Vol. 15, No. 8, 2025, pp. 854. <https://doi.org/10.3390/agriculture15080854>.
- [18] Z. Zhang, Y. Zhang, J. Zhang, Y. Zhu, "Structure, mechanics and material properties of claw cuticle from mole cricket *Grylotalpa orientalis*", *PLOS ONE*, Vol. 14, No. 9, 2019, pp. e0222116. <https://doi.org/10.1371/journal.pone.0222116>.
- [19] Y. S. Bishi, G. Srikanth, L. Hussain, B. Sanduru, R. Chabra, N. Abdurazakova, B. Isakulova, "Design and modal analysis of composite drive shaft for automotive application", *International Conference on Environmental Science, Technology and Engineering (ICESTE 2024)*, Vol. 563, 2024, pp. 02003. <https://doi.org/10.1051/e3sconf/202456302003>.
- [20] D. Novikov, "Application of modal and harmonic analysis to predict the automotive transmission vibration at an early stage of design", *Trudy NAMI*, Vol. 3, 2021, pp. 30-36. <https://doi.org/10.51187/0135-3152-2021-3-30-36>.